JOURNAL OF MATERIALS SCIENCE 29 (1994) 6575–6580

The effects of deposition variables on the spray pyrolysis of ZnO thin film

M.G. AMBIA, M.N. ISLAM, M. OBAIDUL HAKIM*
*Department of Applied Physics and Electronics and * Department of Physics, University of Rajshahi, Rajshahi, Bangladesh*

ZnO thin films were deposited by the spray pyrosol process, and some of their electrical and optical properties have been studied. The as-deposited films are highly resistive, whereas vacuum heat-treated films are good transparent conductors. Optical transmission was found to be more than 96% in between the near infrared and visible region. The ageing effect on these films has been tested.

1. Introduction

Much attention has been paid to ZnO thin films owing to their potential application in various energy-conversion systems. ZnO is non-toxic and chemically stable under normal environmental conditions. ZnO thin films can be prepared by sputtering [1], vacuum evaporation [2], chemical vapour deposition [3] and the spray pyrolysis method [4]. The interest in spray pyrolysis is because of its simplicity and low cost. In our laboratory, we have deposited high-quality undoped ZnO thin films by the pyrosol process using a modified apparatus [5]. In this paper, the effects of some deposition parameters and probable ageing effects on the deposited ZnO films have been reported. The results of optical transmission measurement are also reported.

2. Experimental procedure

Undoped ZnO thin films were deposited by the pyrosol process as described elsewhere [6]. An aqueous solution of zinc acetate (0.4 M) was taken as the ionic solution. All the films were deposited on to glass substrates at a substrate temperature of 360 °C. The measurements were carried out on films 0.1–0.4 μm thick. Thickness was measured by the interferometric method, while resistivity and Hall coefficient were measured by Van der Pauw's method. Structural studies were performed with the electron microscope. Shemadzu UV-180 double-beam spectrophotometer was used for optical studies. All the measurements were performed after a post-deposition heat treatment in vacuum of the order 10^{-5} torr (1 torr = 133.322 Pa) for a period of 1 h at a constant temperature of 250 °C.

3. Results and discussion

3.1. Microstructure

The microstructure of the film was studied with the electron microscope. From these studies it was observed that the orientation of the grains was uniform and the crystallites were very small in size.

3.2. Film-growth activation energy

Fig. 1 shows a plot of log film thickness, t, against $1/T_s$, where T_s is the substrate temperature. By considering the film growth process as a rate process, the activation energy for the film growth was determined from the slope of the plot and was found to be 0.22 eV in the temperature range 270–420 °C.

3.3. The effect of substrate temperature

Fig. 2a shows the plot of resistivity, ρ, versus substrate temperature, T_s, of some as-deposited samples,

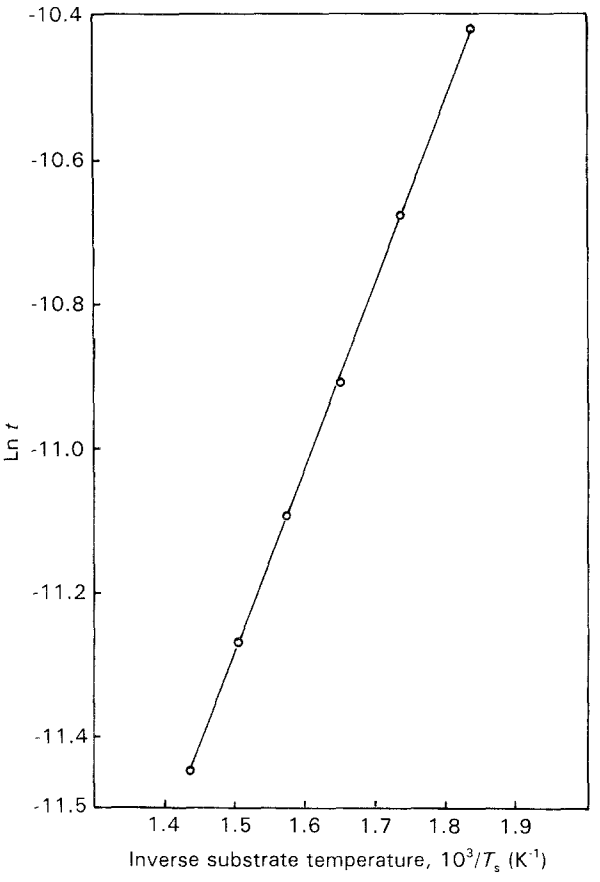

Figure 1 A plot of log film thickness, t, against $1/T_s$ (inverse substrate temperature) of ZnO films.

0022–2461

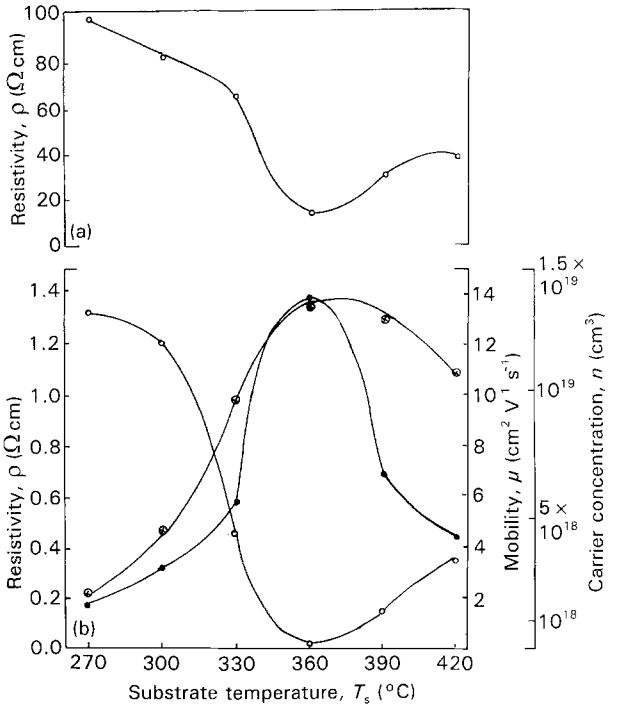

Figure 2 (a) Plot of resistivity, ρ, versus substrate temperature, T_s, of as-deposited ZnO films. (b) A plot of (o) resistivity, ρ, (•) carrier concentration, n, and (⊕) mobility, μ, of vacuum heat treated ZnO films.

whereas Fig. 2b shows the plot of resistivity, ρ, carrier concentration, n, and Hall mobility, μ, of the same set of samples as in Fig. 2a after they were annealed in vacuum.

From Fig. 2a it is observed that the resistivity of the as-deposited samples is very high. The minimum resistivity was found at a substrate temperature of 360 °C, below or above which it began to increase. The nature of the variation of resistivity of as-deposited and vacuum-annealed samples follows the same general sequence, but with a drastically reduced magnitude. The measurement of the Hall coefficient of the as-deposited samples was beyond the scope of our apparatus. The carrier concentration, n, and Hall mobility, μ, follow the same general trend for the vacuum-annealed samples. Starting at lower substrate temperature, the decrease in resistivity is mainly due to increasing n, while for substrate temperature above 360 °C both the carrier concentration and mobility variations cause the increase in ρ. Furthermore, the decrease in μ is probably due to an increase in the grain-boundary barrier heights, whereas the decrease in carrier concentration is perhaps due to relatively better stoichiometry of the films which, in turn, may also increase the resistivity.

It is generally accepted that the n-type conductivity in undoped non-stoichiometric ZnO is due to lattice oxygen deficiency and interstitial zinc atoms, which act as donors [7]. Baumbach and Wagner [8] have ruled out the alternative possibility that vacancies are produced in the oxygen lattice and that the conduction electrons are those which might normally occupy these vacancies by showing that the negative-ion transport number is very small compared with the positive-ion transport number. The small observed positive ionic current is carried either by ionized interstitial zinc atoms or by the normal zinc ions. Because the films are polycrystalline in structure, the resistivity of the as-grown films is very high, possibly because of their grain-boundary effects. During film deposition, a large number of oxygen (O_2^-) molecular ions are chemisorbed and incorporated at the grain boundaries and on the surface of the film, producing potential barriers which hinders the electrical transport. Fujita and Kwan [9] proposed that when these films are heat treated, the chemisorbed O_2^- desorbed from the samples donating an electron in the ZnO ($O_2^- \rightarrow O_2 + e$) hence causing the resistivity to decrease drastically. This is due to a cumulative effect of lowering of grain-boundary potentials and increasing carrier concentration in the sample. On the other hand, in the crystalline lattice, the ions have a closed outer shell and the energy band arises from the filled 2P levels of the O^{2-} ion and empty 4s levels of the Zn^{2+} ion. If the crystal is now caused to lose oxygen by heat treatment, the ions escape as neutral molecules (O_2) leaving behind two electron per atom. They, in turn, combine with the Zn^{2+} ion in an interstitial position to produce a neutral zinc atom. One electron is then easily ionized into the conduction band from the zinc atom in this position [10]. Thus the conductivity of the heat-treated film may easily increase.

3.4. Film thickness

3.4.1. Effect of spray rate on film thickness

The variation of film thickness as a function of spray rate is shown in Fig. 3. The fixed substrate temperature was 360 °C. The variation is not linear. It is seen that, initially, the thickness increases slowly with the spray rate, but at higher spray rate, thickness tends to saturate. At lower spray rate, a smaller quantity of aerosol reaches the substrate, but at a higher spray

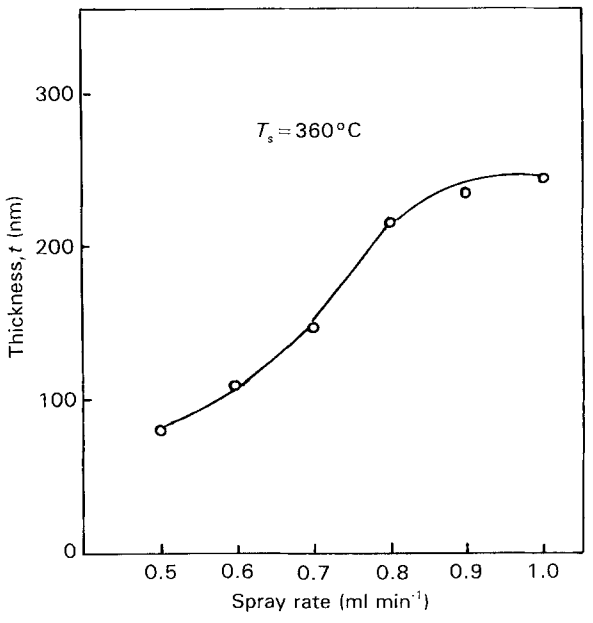

Figure 3 Variation of film thickness as a function of spray rate of ZnO films.

rate, the quantity of reacting aerosol reaching the substrate increases and the thickness of the film increases. However, a time will be reached at a fixed temperature when the reaction rate becomes optimum and further reactant supply could not increase the rate of formation of film; rather the excess reactant will flow outside, remaining unreacted. Therefore, a saturation of film thickness is obtained.

From this observation, the optimum spray rate was found to be about 0.78 ml min^{-1}. With respect to film thickness, better mobility and higher carrier concentration with minimum resistivity (see Fig. 5 below).

3.4.2. The effect of nozzle distance from the substrate

The effect of distance, d, between the substrate and the spray nozzle is shown in Fig. 4, in which a plot of film thickness, t, is shown as a function of d at constant substrate temperature, T_s ($\approx$360 °C). From this plot it is observed that t decreases with the increase in d. At higher distance, the decrease in t is more pronounced. At small d, the maximum amount of vapour molecules which emerge from the nozzle can strike the substrate directly before they become distributed in the reaction chamber. As the nozzle to substrate distance, d, increases, the vapour molecules have sufficient space to distribute laterally in the reaction chamber. As a result, a smaller quantity of the aerosol can reach the substrate, and causes a decrease in deposition rate (thickness). At sufficiently large d($d \approx 30$ cm), the substrate receives no coating, even after a long spraying time. This is obviously due to the vaporization of the aerosol before reaching the substrate.

3.4.3. The effect of spray rate on the resistivity, carrier concentration and mobility

Fig. 5 shows the variation of carrier concentration, n, mobility, μ, and resistivity, ρ, as a function of spray rate. All the films show n-type conductivity in Hall measurement. Both n and μ increase with increasing spray rate and reach maximum around 0.8 ml min^{-1}.

Resistivity, ρ, attains its minimum value at this rate. Above the spray rate of 0.8 ml min^{-1}, n and μ tend to decrease where ρ tends to increase. At higher solution flow rate, the quality of the film becomes poorer. This happens perhaps because of the presence of unreacted species of zinc acetate [11].

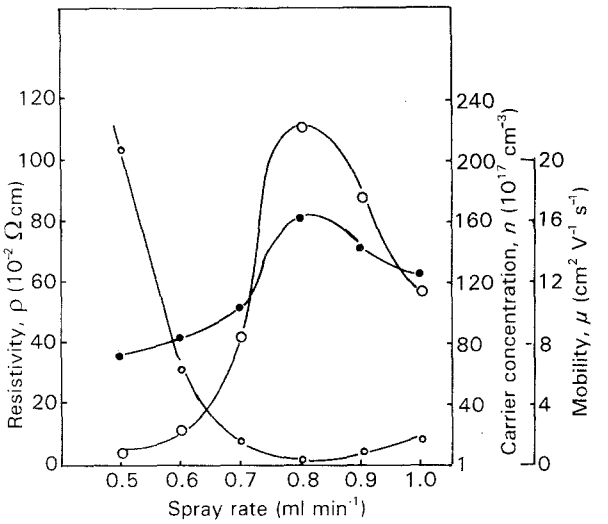

Figure 5 Variation of carrier concentration, n, mobility, μ, and resistivity, ρ, as a function of spray rate of ZnO films.

3.4.4. The dependence of sheet resistance on the film thickness

Fig. 6 shows the dependence of sheet resistance, $R_\square$, on the film thickness. It is observed that sheet resist-

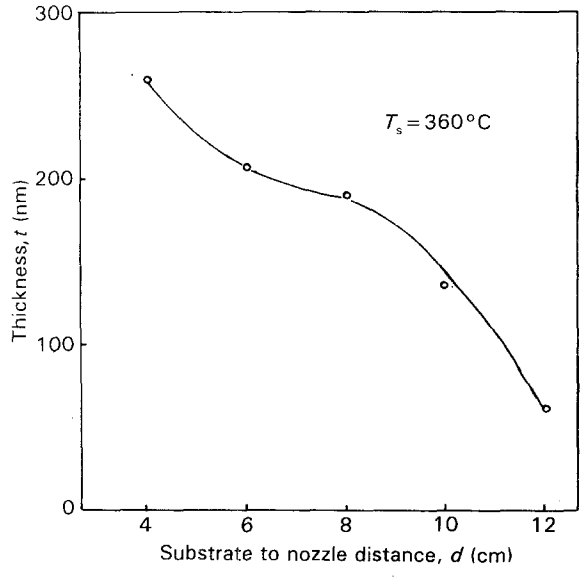

Figure 4 Variation of film thickness, t, as a function of nozzle distance, d (the distance between the substrate and spray nozzle) of ZnO films.

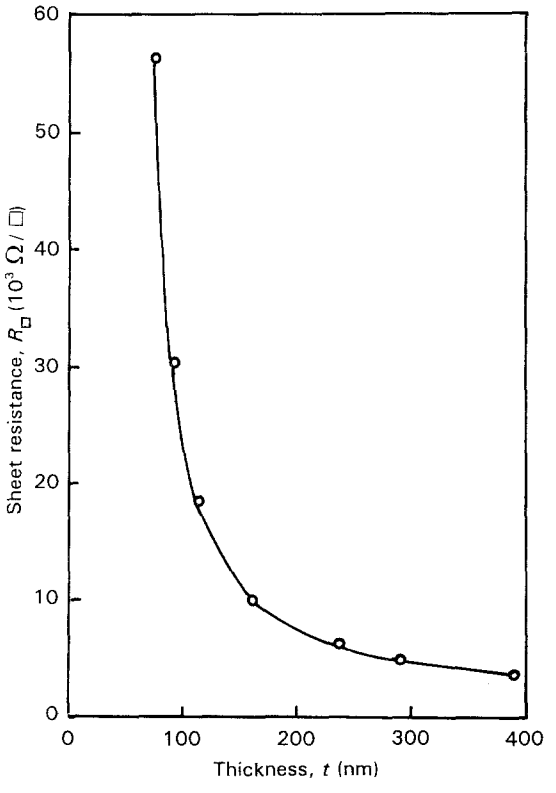

Figure 6 A plot of sheet resistance, $R_\square$, as a function of film thickness, t, of ZnO films.

ance, $R_{\square}$, decreases as the film thickness, t, increases. In the lower range of thickness, a sharp increase in the sheet resistance is observed, but in the higher range of thickness, $R_{\square}$ tends to become almost independent of t. This behaviour is related to the sheet-resistance size effects of spray-deposited films. The effect comes into play in ZnO films significantly only below a thickness of about 150 nm and above this thickness bulk properties may set in [5].

3.4.5. The effect of film thickness on the carrier concentration, mobility and resistivity

Fig. 7 shows the thickness dependence of carrier concentration, n, mobility, μ, and resistivity, ρ, for vacuum-annealed undoped ZnO films. From the figure it is seen that the resistivity, ρ, increases very slowly with decreasing thickness, t, down to 150 nm, below which a sharp increase of ρ is observed.

In the lower range of thickness, n and μ are also very sensitive to the film thickness, t, but in the higher range of t, the dependence is rather feeble. This behaviour may be attributed to the increase in grain size of the film with the increase in film thickness [12]. The increase in resistivity as observed with decreasing film thickness of vacuum-annealed films is mainly due to a decrease in Hall mobility. Major *et al.* [13] suggested that the decrease in mobility is attributed to a decrease in grain size with thickness.

3.5. Ageing effect

Fig. 8 shows the plot of conductivity, σ, against ageing time, T_{da}. Six samples were selected for the experiment. Four of these were undoped and other two were indium-doped. For the undoped samples, the substrate temperatures were different, e.g. for samples 1 and 2 it was 360 °C and for 3 and 4 it was 330 and 300 °C, respectively. For indium-doped samples (5 and 6), the substrate temperature was 360 °C. Their doping concentrations are shown in the figure. Measurements were performed in the open air at room temperature. The samples were previously vacuum heat treated and were kept in an open atmosphere during the observation period. It was found from the figure that 30%–50% of the film's conductivity decreases within 2 weeks for undoped samples, whereas a 20%–30% fall is noticed for indium-doped samples during the same period. After this the film's conductivity remains almost constant for all the samples during the rest of the period.

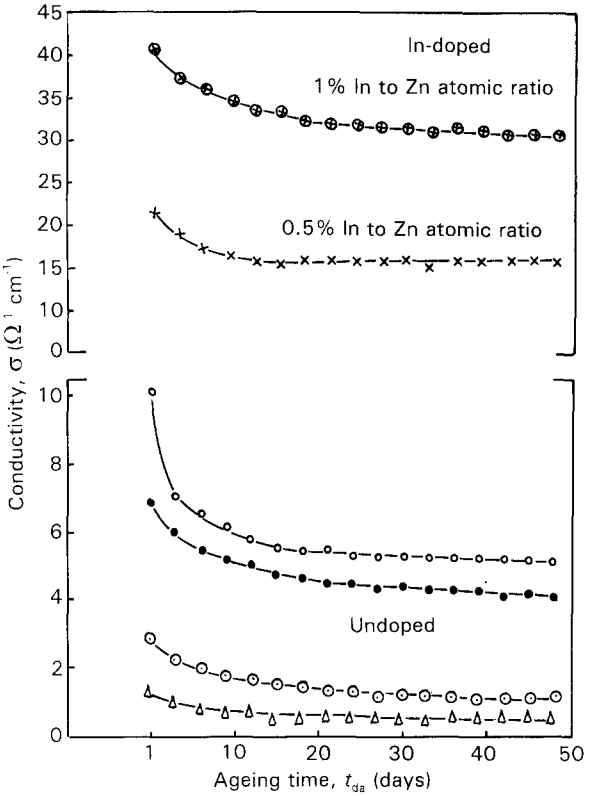

Figure 8 A plot of conductivity, σ, against ageing time T_{da} of ZnO films. Samples: (o) 1, (•) 2, (⊙) 3, (△) 4, (⊕) 5 and (×) 6.

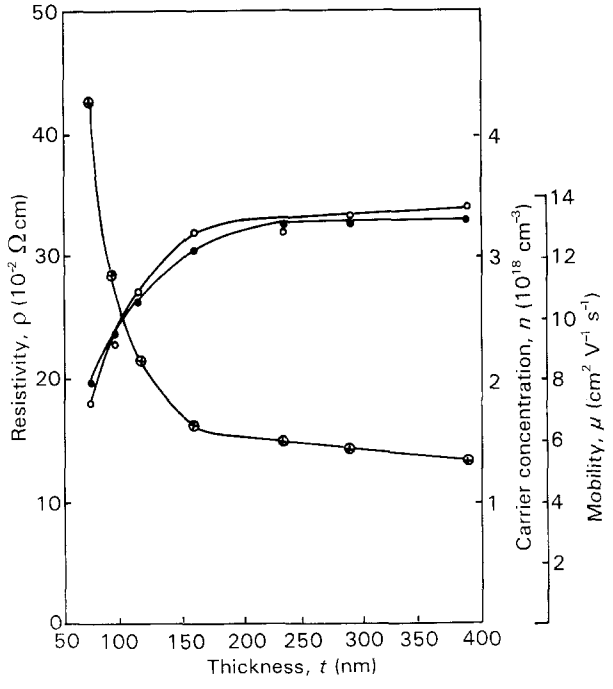

Figure 7 The thickness dependence of (•) carrier concentration, n, (o) mobility, μ, and ⊕ resistivity, ρ, of ZnO films.

Similar observations have been reported by other workers [4, 14, 15]. This decrease in conductivity can be interpreted in terms of oxygen absorption because further heat treatment in vacuum returns the film to its original condition.

3.6. Optical transmission and the band gap

Fig. 9 shows the optical transmission spectra of films of various thicknesses. Measurements were taken in the wavelength range 300–900 nm on both the as-deposited and vacuum heat-treated films. No detectable change was found in the optical transmission due to heat treatment.

The transmission coefficient, T (%) was found to be above 96% at about 540 nm for the films of thickness below 200 nm, above which a decrease in transmission is observed. All the samples were found to show a sharp ultraviolet cut-off at about 370 nm.

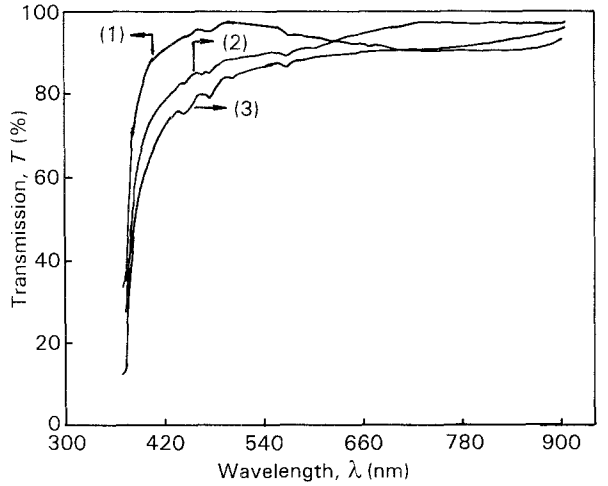

Figure 9 A plot of transmission, T versus wavelength of ZnO films, for t: (1) 100 nm, (2) 150 nm, (3) 390 nm.

The refractive index was calculated from the transmission data. The values of refractive index lie between 1.57 and 2.05 at about 460 nm in the visible range of the optical spectra. Higher values of refractive indices were also obtained in the films of higher thickness. The values obtained agreed well with the reported value of 2 for ZnO crystal [16]. Because the ZnO films are found to be highly transparent between the visible to near infrared region, the reflection coefficient, R, can thus be neglected in calculating the absorption coefficient in the region. The absorption coefficient, α, can be directly determined from the transmission spectra using the relation

$$\alpha = \frac{\ln(1/T)}{t} \quad (1)$$

where t is the film thickness and T is the transmittance. Assuming that the transition probability becomes constant near the absorption edge, the absorption coefficient, α, for direct allowed transition for a simple parabolic band scheme can be described as a function of incident photon energy, $h\nu$, as

$$\alpha \propto (h\nu - E_g)^{\frac{1}{2}} \quad (2)$$

where E_g is the optical band gap. Fig. 10 shows the plot of $(\alpha h\nu)^2$ against $h\nu$ for a few samples with different carrier concentrations having the same thickness. The values of E_g have been determined by extrapolating the linear portion of the curves to the zero absorption line.

It is observed from Fig. 10 that the fundamental absorption edge gradually shifts towards higher energies (shorter wavelength) with increasing carrier concentration. This effect of widening of the band-gap is attributed primarily to the Burstein–Moss shift in semiconductor [17, 18], but more detailed analysis has been presented elsewhere [19]. It is noticed from this Fig. 10 that the values of $E_g = 3.21$ eV at a carrier concentration of 9.58×10^{17} cm^{-3} increases up to 3.3 eV for a sample with carrier concentration of 1.38×10^{19} cm^{-3}. These values are in good agreement with the reported values [20, 7, 21]. The variation of

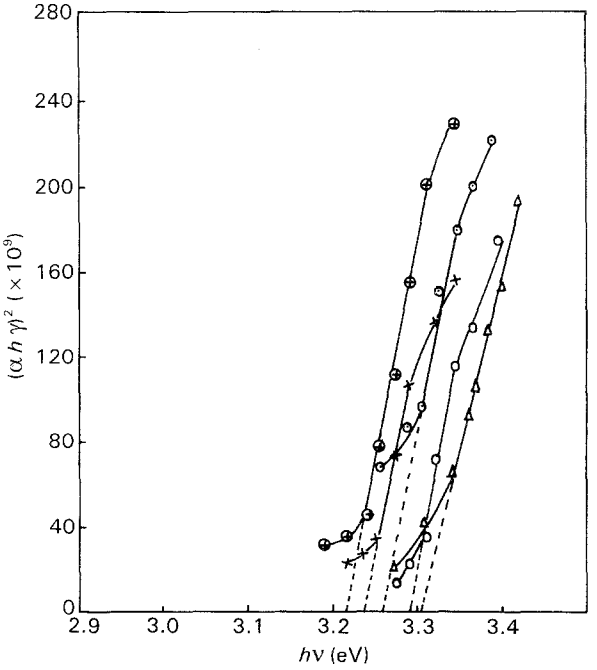

Figure 10 Plot of $(\alpha h\nu)^2$ versus $h\nu$ showing the shift of the absorption edge with respect to the carrier concentration, n (cm^{-3}) of ZnO films. (⊕) $n = 9.58 \times 10^{17}$ cm^{-3}; (×) $n = 2.41 \times 10^{18}$ cm^{-3}; (⊙) 3.62×10^{18} cm^{-3}; (○) 8.31×10^{18} cm^{-3} (△) 1.38×10^{19} cm^{-3}.

E_g with film thickness was not noticeable. No remarkable ageing effect on E_g was observed.

3.7. Figure of merit of the layer

The figure of merit, ϕ_{TC} (where $\phi_{TC} = T^{10}/R_{\square}$), as presented by Haacke for a transparent conductor, has been calculated for these films. Highest ϕ_{TC} was obtained to be $0.64 \times 10^{-4}\ \Omega^{-1}$ for a film of thickness 174.2 nm. A variation of sheet resistance, $R_{\square}$, with optical transmission, T, at three different wavelengths in the visible region is presented in Fig. 11. This implies no significant variation of optical transmission with sheet resistance except in the lower wavelength limit.

4. Conclusions

1. The conductivity of as-deposited undoped ZnO films is poor, whereas vacuum heat-treated films are excellent conductors.

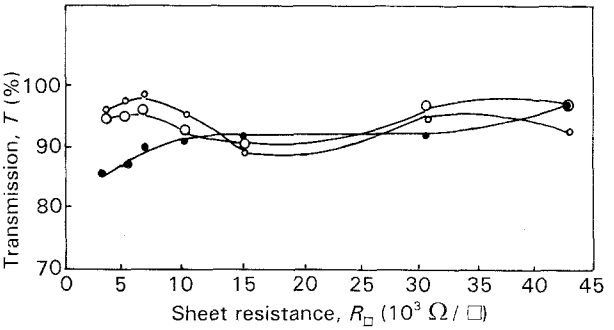

Figure 11 A plot of transmission, T (%) versus sheet resistance at three different wavelengths: (●) 460 nm (○) 560 nm (o) 660 nm.

2. The film's properties are found to depend remarkably on the deposition system.

3. Some change of the film's conductivity was observed due to the ageing effect but is limited to within the first 2 weeks of the deposition.

4. The magnitude of the band-gap is similar to that of the pure bulk crystal, although these films were impure and full of structural defects.

References

1. J. C. YEN, *J. Vac. Sci. Technol.* **12** (1975) 47.
2. E. MOLLWO, *Ann. Phys.* **6** (1948) 230.
3. M. KASUGA and S. ISHIHARA, *Jpn J. Appl. Phys.* **15** (1976) 1835.
4. JULIO ARANOVICH, ARMANDO ORTIZ and RICHARD H. BUBE, *J. Vac. Sci. Technol.* **16** (1979) 994.
5. M. N. ISLAM and M. O. HAKIM, *J. Phys. Chem. Solids* **46** (1985) p. 339.
6. M. N. ISLAM, M. O. HAKIM and H. RAHMAN, *J. Mater. Sci.* **22** (1987) 1379.
7. A. P. ROTH and D. F. WILLIAMS, *J. Appl. Phys.* **52** (1981) 6686.
8. H. H. V. BAUMBACH and C. WAGNER, *Z. Phys. Chem.* **22B** (1933) 199.
9. Y. FUJITA and T. KWAN, *J. Res. Inst. Catal.* **7** (1959) 24.
10. LEONID V. AZAROFF and JAMES J. BROPHY, "Electronic process in materials" (McGraw-Hill, New York, 1963) p. 234.
11. S. MAJOR, A. BANERJEE and K. L. CHOPRA, *Thin Solid Films* **108** (1983) 333.
12. *Idem, ibid.* **125** (1984) 179.
13. *Idem, ibid.* **143** (1986) 19.
14. L. BAHADUR, M. HAMDANI, J. F. KOENIG and P. C HARTIER, *Solar Energy Mater.* **14** (1986) 107.
15. C. X. QIU and I. SHIH, *ibid.* **13** (1986) 75.
16. E. MOLLWO, in "Photoconducting Conference" (Wiley, New York, 1956).
17. E. BURSTEIN, *Phys. Rev.* **93** (1954) 632.
18. T. S. MOSS, *Proc. Phys. Soc. Lond.* **B67** (1954) 775.
19. I. HAMBERG and C. G. GRANQVIST, K.-F. BERGGREN, B. E. SERNELIUS and L. ENGSTROM, *Solar Energy Mater.* **12** (1985) 479.
20. H. GERISCHER and F. WILLING, "Topics in Current Chemistry 61" (Springer, Berlin-Heidelberg, 1976) p. 31.
21. CHRIS EBRSPACHER, ALAN L. FAHRENBRUCH and RICHARD BUBE, *Thin solid films* **136** (1986) 1.

Received 10 March 1993
and accepted 16 May 1994